

Supplementary data

Inducing hair follicle neogenesis with secreted proteins enriched in embryonic skin

Sabrina Mai-Yi Fan, Chia-Feng Tsai, Chien-Mei Yen, Miao-Hsia Lin, Wei-Hung Wang, Chih-Chieh Chan, Chih-Lung Chen, Kyle K.L. Phua, Szu-Hua Pan, Maksim V. Plikus, Sung-Liang Yu, Yu-Ju Chen, and Sung-Jan Lin

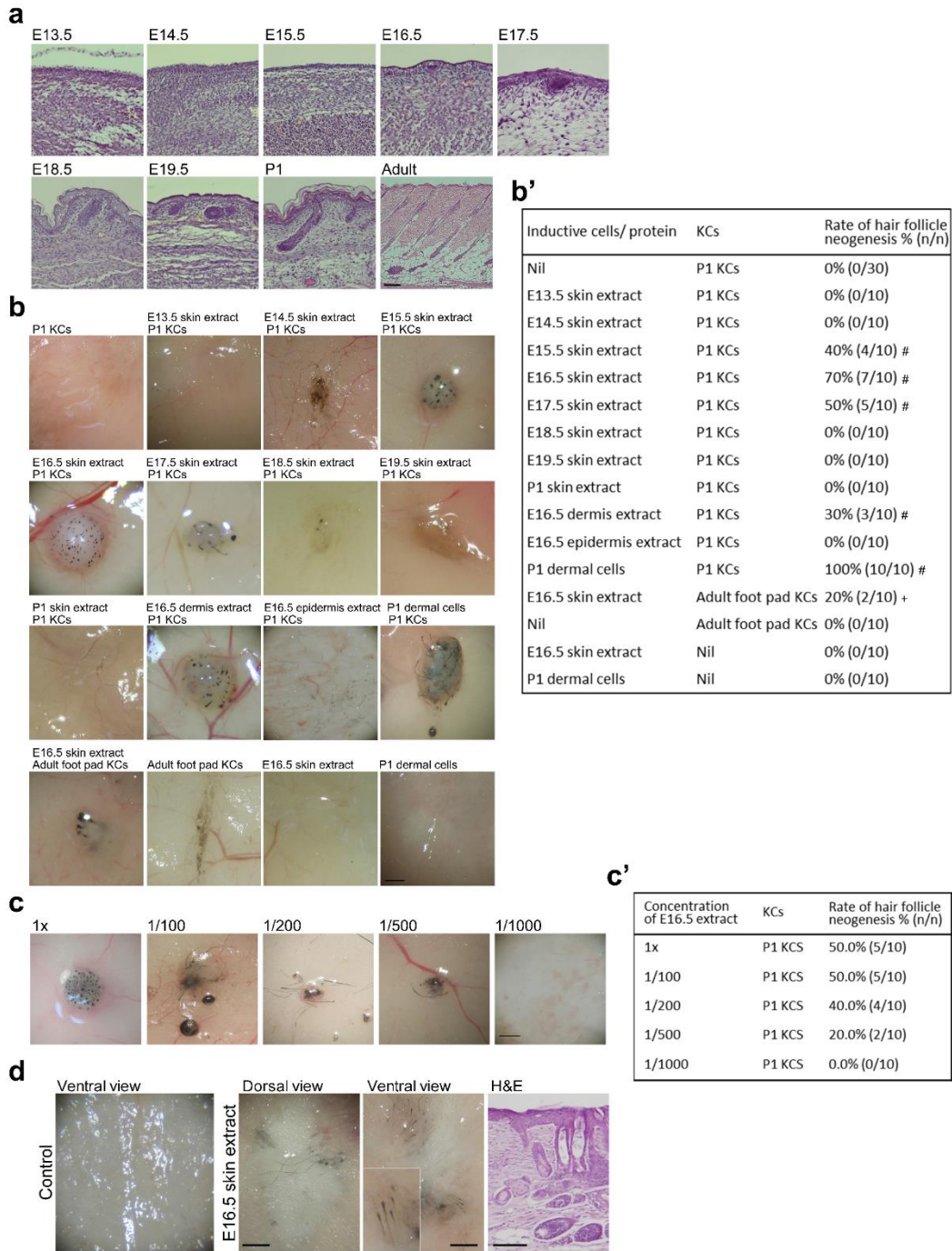


Figure S1. The effect of cell-free whole-skin extract prepared from different developmental stages on HF neogenesis. (a) Histology of Wistar rat skin at different developmental stages. In Wistar rats, embryonic HF development is delayed by ~1–1.5 days compared with mice. At E15.5, early hair placodes can be observed. Formation of hair germs with dermal condensates proceeds on E17.5. HFs develop to the short hair peg stage on E18.5. **(b-b')** Effect of cell-free whole-skin extract on HF neogenesis. **(b)** Representative results of patch assays. **(b')** Summary of patch assay results. Cell-free extracts from E15.5–17.5 whole skin induced new HFs from P1 KCs. For E16.5 skin,

dermal extract, but not epidermal extract, was able to induce HF neogenesis from P1 KCs, indicating that factors present in the dermis were sufficient to induce new HFs. E16.5 skin extract also induced HF neogenesis from adult KCs derived from hairless footpad skin (+ $p = 0.0767$). # $p < 0.05$, compared with P1 KCs only. **(c-c')** The effect of serial dilution of E16.5 skin extract on HF inductivity. **(c)** Representative results of patch assays. **(c')** Summary of patch assay results. E16.5 skin extract was serially diluted from 1 $\mu\text{g}/\mu\text{l}$ (1 \times) to 1×10^{-3} $\mu\text{g}/\mu\text{l}$ (1/1000). Upon serial dilution, E16.5 skin extract gradually lost its ability to induce HFs, which disappeared completely by the 1/1000 dilution. **(d)** Effect of E16.5 extract on full-thickness wounds. In full-thickness wounds of nude mice, locally administered E16.5 extract induced HF neogenesis from transplanted C57BL/6 mouse keratinocytes (n=3). KC: keratinocyte. Bar: 100 μm in histology, 500 μm in gross images.

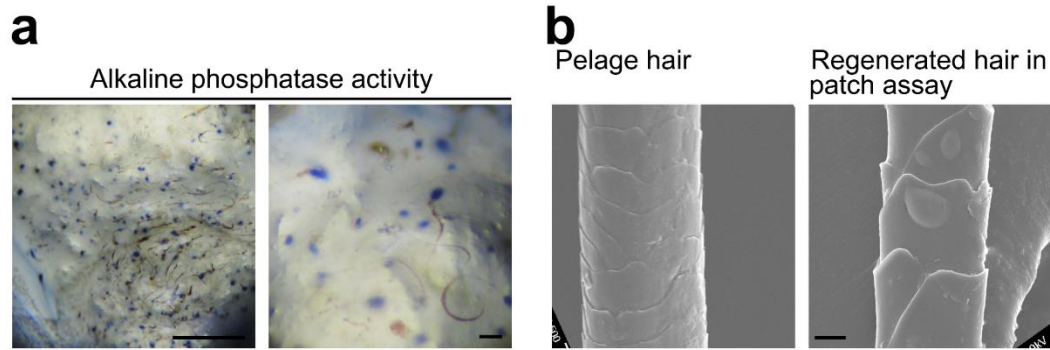


Figure S2. Alkaline phosphatase activity and hair shaft morphology of new HFs induced by E16.5 skin extract. (a) New HFs in patch assays exhibited alkaline phosphatase activity (blue color) in the proximal hair bulbs, marking new DPs. The right panel shows a magnified view. (b) Scanning electron micrographs of normal pelage hair and newly regenerated hair, both showing overlapping cuticles covering the hair shafts. Bar: 100 μm in (a), 10 μm in (b).

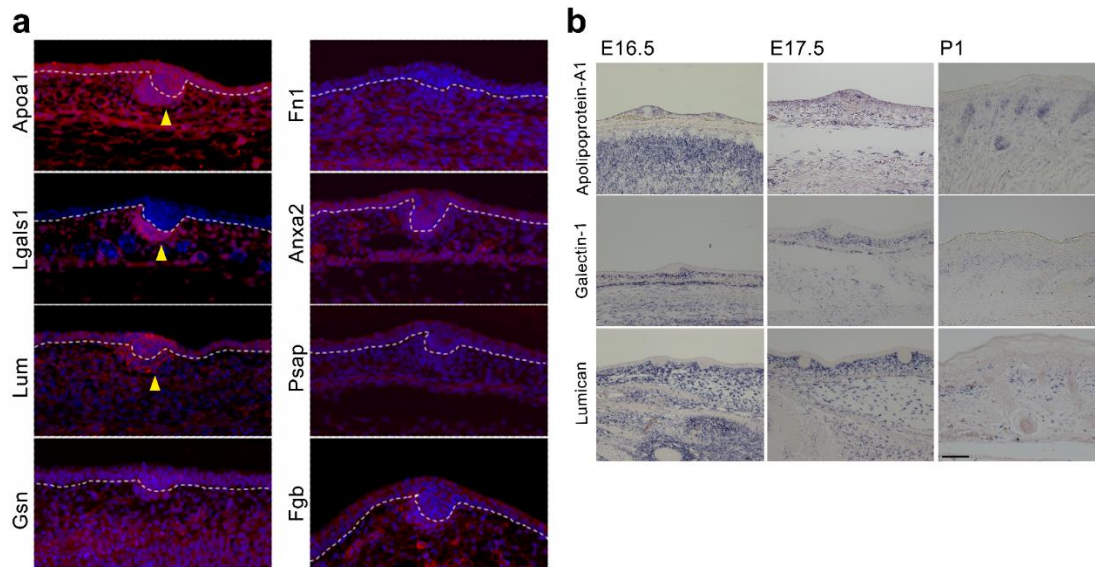


Figure S3. Expression of specific proteins in rat embryonic skin. (a) Immunostaining for the eight proteins in E17.5 Wistar rat embryonic skin. Compared with the seven other proteins, galectin-1 is preferentially localized to the dermis. Apolipoprotein-A1, galectin-1 and lumican are also abundant in the dermal condensate (yellow arrowheads) of the developing HFs. Red: specific protein; blue: nuclear DAPI staining; dashed line: basement membrane. (b) *In situ* hybridization for the expression of apolipoprotein-A1, galectin-1 and lumican genes in the skin at different stages. All three genes are highly expressed in the mesenchyme of E16.5 and E17.5 embryonic skin. Expression of apolipoprotein-A1 in the epithelium was also observed in E16.5 and E17.5 skin. The expression level for all three genes in the dermis diminishes in P1 skin. Bar: 100 μ m.

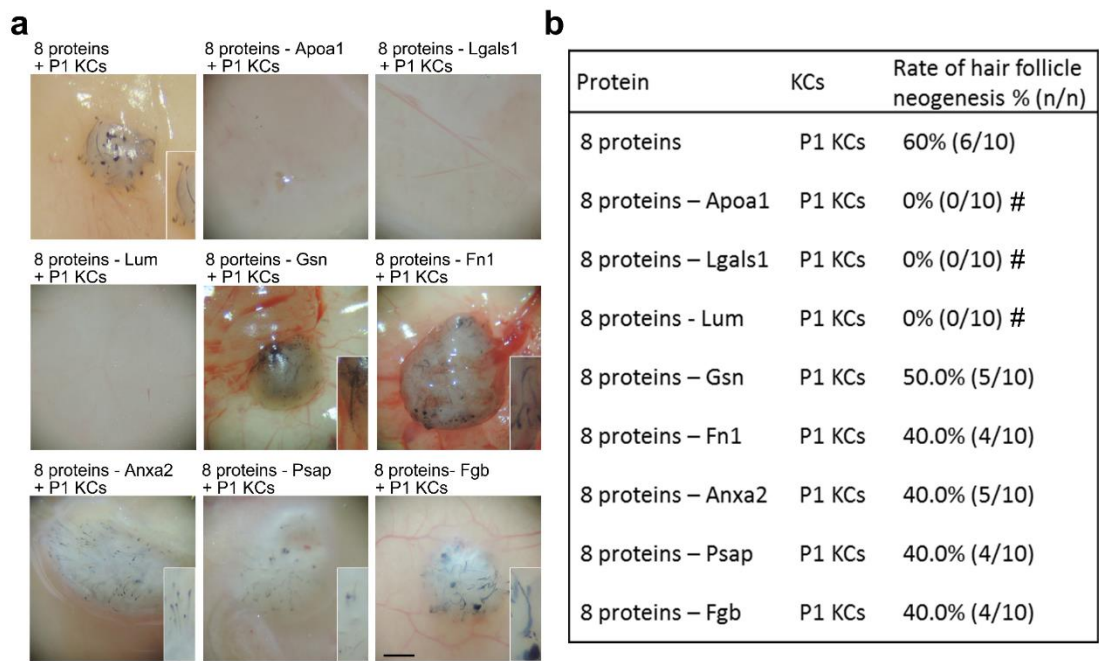


Figure S4. Seven- or eight-protein combinations induce HF neogenesis. (a) Representative patch assays. Bar: 500 μ m. **(b)** Summary of patch assay results. Removal of Apoa1, Lgals1 or Lum from the eight-protein mixture ablated the ability to induce HF neogenesis. # $p < 0.05$, compared with the eight-protein mixture (n=10).

Table S1

Liquid chromatography-tandem mass spectrometry (LC-MS/MS) analysis of proteomes of E16.5 and P1 skin extract.

Table S2

RNA sequencing data of adult murine fibroblasts after exposure to E16.5 skin extract, ApoA1/Lgals1/Lum mix or each of the 3 proteins, murine E14.5 dermal fibroblasts and murine dermal papilla cells. Folds changes of gene expression in comparison with adult dermal fibroblasts were shown.

Table S3

Top 20 upregulated cellular processes in adult murine fibroblasts cultured in E16.5 extract, Apoa1/Lgals1/Lum mix, Apoa1, Lgals1, and Lum.

Cellular processes shown in bold type indicate the ones shared with E16.5 extract treatment.

E16.5 extract	Apoa1/Lgals1/Lum mix	Apoa1	Lgals1	Lum
Pathways in cancer	Pathways in cancer	Pathways in cancer	Pathways in cancer	Pathways in cancer
Focal adhesion	MAPK signaling	MAPK signaling	MAPK signaling	Cytokine-cytokine receptor interaction
Regulation of actin cytoskeleton	Focal adhesion	Cytokine-cytokine receptor interaction	Cytokine-cytokine receptor interaction	MAPK signaling
MAPK signaling	Regulation of actin cytoskeleton	Ribosome	Ribosome	Focal adhesion
Chemokine signaling	Chemokine signaling	Regulation of actin cytoskeleton	Focal adhesion	Regulation of actin cytoskeleton
Axon guidance	Endocytosis	Focal adhesion	Regulation of actin cytoskeleton	Ribosome
Endocytosis	Calcium signaling	Chemokine signaling	Chemokine signaling	Chemokine signaling
Ubiquitin mediated proteolysis	Axon guidance	Calcium signaling	Leukocyte transendothelial migration	Jak-STAT signaling
Wnt signaling	Wnt signaling	Axon guidance	Neurotrophin signaling	Axon guidance
Insulin signaling	Tight junction	Leukocyte transendothelial migration	Axon guidance	Neurotrophin signaling
TGF-beta signaling	Neurotrophin signaling	Neurotrophin signaling	ECM-receptor interaction	Leukocyte transendothelial migration
Neurotrophin signaling	Insulin signaling	B cell receptor signaling	T cell receptor signaling	Lysosome
Tight junction	Vascular smooth muscle contraction	ECM-receptor interaction	Small cell lung cancer	Toll-like receptor signaling

Lysosome	Leukocyte transendothelial migration	T cell receptor signaling	Vascular smooth muscle contraction	Natural killer cell mediated cytotoxicity
Cell cycle	Ubiquitin mediated proteolysis	Vascular smooth muscle contraction	Oocyte meiosis	ECM-receptor interaction
Small cell lung cancer	Cell cycle	Natural killer cell mediated cytotoxicity	Fc gamma R-mediated phagocytosis	T cell receptor signaling
Prostate cancer	Melanogenesis	Lysosome	B cell receptor signaling pathway	Vascular smooth muscle contraction
ECM-receptor interaction	GnRH signaling pathway	Small cell lung cancer	Toll-like receptor signaling pathway	VEGF signaling
Melanogenesis	Gap junction	VEGF signaling	Fc epsilon RI signaling	B cell receptor signaling
Gap junction	ErbB signaling	Fc epsilon RI signaling	NOD-like receptor signaling	Hematopoietic cell lineage